

1 **Elucidating the competition between heterotrophic denitrification and**  
2 **DNRA using the resource-ratio theory**

3

4 **Mingsheng Jia<sup>1</sup>, Mari K.H. Winkler<sup>2</sup>, Eveline I.P. Volcke<sup>1,\*</sup>**

5 1. Department of Green Chemistry and Technology, Ghent University, Coupure links 653,  
6 9000 Gent, Belgium

7 2. Department of Civil and Environmental Engineering, University of Washington, Seattle,  
8 WA 98195-2700, USA

9 \*Corresponding author: [Eveline.Volcke@UGent.be](mailto:Eveline.Volcke@UGent.be)

10

11

12

13

14 **Abstract**

15 Denitrification and dissimilatory nitrate reduction to ammonium (DNRA) are two microbial  
16 processes competing for nitrate and organic carbon (COD). Their competition has great  
17 implications for nitrogen loss, conservation, and greenhouse gas emissions. Nevertheless, a  
18 comprehensive and mechanistic understanding of the governing factors for this competition is  
19 still lacking. We applied the resource-ratio theory and verified it with competition  
20 experiments of denitrification and DNRA reported in the literature. Based on this theory, we  
21 revealed how COD/N ratio, influent resource concentrations, dilution rate, and stoichiometric  
22 and kinetic parameters individually and collectively define the boundaries for different  
23 competition outcomes in continuous cultures. The influent COD/N ratio alone did not drive  
24 competition outcome as the boundary COD/N ratio for different competition outcomes  
25 changed significantly with influent resource concentrations. The stoichiometry of the two  
26 processes was determinative for the boundaries, whereas the affinity for the resources ( $K_s$ ),  
27 maximum specific growth rate ( $\mu_{max}$ ) of the two species and the dilution rate had significant  
28 impacts as well but mainly at low influent resource concentrations (e.g., <100  $\mu$ M nitrate).  
29 The proposed approach allows for a more comprehensive understanding of the parameters  
30 controlling microbial selection and explains apparently conflicting experimental results. The  
31 results from this model also provide testable hypotheses and tools for understanding and  
32 managing the fate of nitrate in ecosystems and for other species that compete for two  
33 resources.

34 **Keywords:** Nitrate reduction; Chemostat; Resource concentration; COD/N ratio; Dilution  
35 rate; Mathematic model

36

## 37 **1. Introduction**

38 Denitrification (DEN) and dissimilatory nitrate reduction to ammonium (DNRA, also termed  
39 as dissimilatory/respiratory/nitrate ammonification) are two main microbial processes  
40 competing for nitrate as an electron acceptor [1]. During denitrification, nitrate is converted to  
41 nitrogen gas, thereby leading to nitrogen loss in natural and engineered ecosystems such as  
42 wastewater treatment plants (WWTPs). Nitrous oxide, a potent greenhouse gas, can be  
43 emitted during this process, posing an increasing concern [2]. In contrast, DNRA retains  
44 nitrogen locally by converting nitrate to bioavailable ammonium, which may be beneficial for  
45 natural ecosystems but unwanted for WWTPs [3]. Besides, DNRA seems not to contribute to  
46 N<sub>2</sub>O emissions [1]. Growing evidence suggests that DNRA can be significant in both aquatic  
47 and terrestrial ecosystems [4, 5]. Nevertheless, little is known about the importance of DNRA  
48 and its relative contribution to global N-cycling [1, 6, 7]. Therefore, there is a pressing need to  
49 better comprehend the factors influencing the competition between denitrification and DNRA  
50 for nitrate.

51 Energetics and kinetics are the general physiological features of microorganisms that  
52 explain and regulate the outcome of competition [8]. Theoretically, the catabolic reaction of  
53 the denitrification pathway yields more free energy per unit of organic carbon oxidized (e.g.,  
54 802 vs. 505 kJ per mole acetate) whereas for the DNRA pathway slightly more free energy is  
55 liberated per unit of nitrate reduced (505 vs. 501 kJ per mole nitrate with acetate as electron  
56 donor) [3, 9]. Moreover, the biomass yield per mole nitrate is 0.2-2 times higher from the  
57 DNRA process than that of the DEN process [3, 9]. Therefore, from a thermodynamic  
58 standpoint, it can be justified that DEN should occur under organic carbon-limiting conditions  
59 (i.e., low COD/N), while DNRA is promoted under nitrate-limiting conditions (i.e., high  
60 COD/N) [3, 10–12]. In addition, Tiedje [12] proposed a theory that high labile carbon  
61 availability would favor organisms that use electron acceptors most efficiently; DNRA

62 transfers eight electrons per mole of nitrate reduced, whereas denitrification only transfers  
63 five. According to this theory, DNRA should be more efficient and abundant under nitrate-  
64 limiting conditions. Previous studies also suggest that DNRA bacteria generally have a lower  
65 maximum specific growth rate but a higher affinity for nitrate compared to denitrifiers [8, 13].  
66 The higher affinity for nitrate may also explain the observed dominance of DNRA over  
67 denitrification under nitrate-limiting conditions [13]. In opposition to the theoretical  
68 explanations that suggest DNRA dominance under nitrate-limiting conditions, results have  
69 shown that high COD/N ratios do not necessarily lead to a shift from DEN to DNRA [14, 15].

70         Apart from energetics and kinetics, environmental conditions affect the biological  
71 nitrate partitioning as well. There are multiple studies suggesting that the competition depends  
72 on the dilution rate [11, 16] and initial resource concentration [8]. In addition, other studies  
73 conducted with a pure culture that encompasses a dual pathway showed that COD/N ratio  
74 alone was insufficient to explain pathway selection as at low resource concentrations the  
75 culture disproportionately utilizes DNRA rather than denitrification [17]. These results  
76 delineate that a comprehensive understanding of the factors that drive the partitioning or  
77 coexistence of both pathways is lacking, and a mathematical approach to explain competition  
78 outcome may be helpful.

79         Over the years, theoretical frameworks have been developed to predict the outcome of  
80 interspecies microbial competition for the same resources. One example is the resource-ratio  
81 theory, which describes the interactions between resources and growth of two or more  
82 competing species and can predict the outcomes of microbial competition for resources, in  
83 advance of actual competition experiments [18–20]. This theory takes both physiological  
84 properties and environmental conditions into account. It has been successfully demonstrated  
85 in predicting the outcome of microbial competition for a single nutrient [21] as well as in an  
86 ecological competition between algae for two resources (phosphate and silicate) [22]. The

87 analytical solutions of generalized competition scenarios in continuous systems (e.g.,  
88 chemostat) have been investigated at steady state, and results revealed survival of one or  
89 coexistence of both species at given circumstance (e.g., [19, 23]).

90 This study investigates the potential of the resource-ratio theory in elucidating the  
91 competition between denitrification and DNRA. More specifically, it is studied whether this  
92 mathematical approach can match and explain the underlying principle for the seemingly  
93 conflicting measurements conducted at different COD/N ratios in different studies. To this  
94 end, the resource-ratio theory was applied to predict the experimental competition outcome of  
95 heterotrophic denitrifiers and DNRA bacteria in continuous cultures [3, 13]. After verification,  
96 the theory was used to test different conditions to understand what may drive pathway  
97 partitioning or coexistence. The results highlight the impact of COD/N ratio, resource  
98 concentrations, dilution rate, and microbial stoichiometric and kinetic parameters on the  
99 competition outcome. Moreover, a generalized spreadsheet was created and supplied to ease  
100 the application of this mechanistic theory to similar competition scenarios.

101

## 102 **2. Materials and methods**

103 After introducing the basics of the resource-ratio theory (section 2.1), this theory was  
104 implemented to predict the competition outcome of heterotrophic denitrification and DNRA  
105 (section 2.2). Its applicability was subsequently evaluated with experimental data available  
106 from literature case studies [3, 13] (section 2.3).

### 107 **2.1 The resource-ratio theory**

108 The resource-ratio theory describes the interaction between resources and growth of  
109 competing species and enables to predict the outcome of microbial competition for shared  
110 resources, instead of or prior to actual competition experiments [18, 19]. The growth of the  
111 microorganisms on the limiting resources was assumed to follow Monod kinetics (Eq. 1) [24].

$$\mu_i = \mu_{max,i} \frac{S}{K_{S_i} + S} \quad (1)$$

112 Where  $\mu_i$  is the specific growth rate of species  $i$  ( $\text{h}^{-1}$ );  $\mu_{max,i}$  is the maximum specific growth  
113 rate of species  $i$  ( $\text{h}^{-1}$ );  $K_{S_i}$  is the half-saturation constant (i.e., affinity constant) of species  $i$  for  
114  $S$  ( $\mu\text{M}$ );  $S$  is the concentration of resource  $S$  ( $\mu\text{M}$ ).

115 For every limiting resource in a continuous system, there is a subsistence resource  
116 concentration at which the growth rate balances the dilution rate ( $D$ ), which is defined as the  
117 parameter  $J_S$  (Eq. 2).  $J_S$  also represents the concentration of resource  $S$  at steady state [25].  
118 Below this concentration, the net growth rate would be negative, and thus, the species cannot  
119 sustain. If  $n$  species are competing for a single limiting resource ( $S$ ), the species  $i$  with the  
120 lowest subsistence resource concentration  $J_{S_i}$  can utilize the limiting resource to the lowest  
121 level at a given dilution rate and influent resource concentration and thus is the only possible  
122 winner at steady-state. This has been previously proven mathematically [25] and  
123 experimentally [21].

124

$$J_{Si} = K_{Si} \cdot \frac{D}{r_{Si}} = K_{Si} \cdot \frac{D}{\mu_{max,i} - D} \quad (2)$$

125 Where  $J_{Si}$  is the subsistence concentration of growth-limiting resource S for species i ( $\mu\text{M}$ ); D  
126 is the dilution rate ( $\text{h}^{-1}$ );  $r_{Si}$  is the intrinsic growth rate and equals to  $(\mu_{max,i} - D)$  ( $\text{h}^{-1}$ );

127 The competition of two species (N1 and N2) for two resources (S and R) in a  
128 continuous culture is illustrated in Fig. 1, following a graphical-mechanistic approach that  
129 was developed to study the competition and predation in macroecology [18]. In this two  
130 resources plane (Fig. 1), for every species i, the so-called ‘Zero Net Growth Isoclines’ (ZNGIs)  
131 are drawn, which are defined by the subsistence resource concentrations (i.e. J parameter) for  
132 the two complementary resources. A species i cannot survive outside the boundary ZNGIs,  
133 i.e., for  $S < J_{Si}$  and/or  $R < J_{Ri}$ , even in the absence of a competing species. Stable coexistence  
134 only occurs when the ZNGIs of the two species coincide (as in Fig.1), i.e. when each species  
135 has lower subsistence concentration (J) for one of the two resources. If the ZNGIs of two  
136 competing species do not cross, it means one species must have lower J parameters for both of  
137 the two resources, and as a result it would always win the competition [18, 19]. Moreover, it  
138 is assumed that the growth is restricted by the most limiting resource (i.e., the one that results  
139 in lower growth rate in Eq.1), as described by Eq. 3 [19]. To maintain an equilibrium  
140 population, the resource consumption rate must balance the resource supply rate. The  
141 consumption vector (defined as  $C_i$ , Eq.4 and in Fig. 1) and the ZNGIs define the regions in  
142 which either one of the two dominates or two species coexist (Fig. 1). The model based on  
143 this theory was further detailed in the Supplementary Information (SI, section S1).

$$\mu_i(S, R) = \min \left( \mu_{max,i} \frac{S}{K_{Si} + S}, \mu_{max,i} \frac{R}{K_{Ri} + R} \right) \quad (3)$$

$$C_i = \frac{Y_{Si}}{Y_{Ri}} \quad (4)$$

144 Where  $Y_{Si}$ ,  $Y_{Ri}$  are the yield of species  $i$  per unit of resource  $S$  or  $R$  consumed (mole biomass  
145 per mole  $S$  or  $R$ ); therefore  $C_i$  represents the ratio of the consumption of resource  $R$  to  
146 resource  $S$  by species  $i$  (mole  $R$  per mole  $S$ ).

147 Overall, with kinetic and stoichiometric parameters of the competing species (e.g.  
148  $\mu_{max}$ ,  $Ks$  and  $Y$ ) and environmental conditions (e.g., influent resource concentration and  
149 dilution rate), the resource-ratio theory enables to qualitatively and quantitatively predict the  
150 competition outcomes, the status of the competing species and resources (e.g., concentrations)  
151 at steady state (i.e., equilibrium points) and the dynamic (i.e. how the steady state is reached).

## 152 **2.2 Application of the theory for the competition between denitrification and DNRA**

153 In this study, heterotrophic denitrification and DNRA were assumed to be carried out by two  
154 distinct specialist species and directly compete for nitrate and organic carbon (COD, e.g.,  
155 acetate). Their competition in continuous culture (i.e., chemostat) can be regarded as a  
156 specific case of the general resource-ratio theory for two species competing for two resources  
157 (Fig. S1). The kinetic and stoichiometric parameters used in this study for the application of  
158 this theory are presented in Table S2.

159 These values were used as the default (i) to verify the theory (section 3.1), (ii) to  
160 analyze the impact of influent resource concentration and dilution rate on the boundary  
161 COD/N ratios and thus the competition outcome (section 3.2 and 3.3), and (iii) to study the  
162 dynamic system behaviour (section 3.5). To date, kinetic and stoichiometric parameters (e.g.,  
163  $Y$ ,  $\mu_{max}$ , and  $Ks$ ) of heterotrophic DNRA microorganisms have only been limitedly reported.  
164 Therefore, a local sensitivity analysis was performed to investigate the potential impact of  
165 these parameters on the competition outcome (section 3.4).



166 **2.3 Experimental case studies for theory verification**

167 To verify the resource-ratio theory, two experimental studies on the competition between  
168 heterotrophic denitrification and DNRA processes by van den Berg et al. [3, 13] were used. In  
169 these studies, chemostat enrichment cultures were fed with different levels of acetate and  
170 nitrate (COD/N=1.8-8.5 g COD g N<sup>-1</sup>), with an averaged dilution rate of 0.026 h<sup>-1</sup>. The  
171 experimental conditions, observed competition outcomes, and measured biomass  
172 concentrations at steady state are summarized in Table S3.

### 173 **3. Results and discussion**

#### 174 **3.1 Verification of the resource-ratio theory**

175 This study used the results from two previously published chemostat enrichment cultures as  
176 case studies for theory verification [3, 13]. These cultures were fed with different levels of  
177 acetate and nitrate (COD/N=1.8-8.5 g COD g N<sup>-1</sup>, Table S3). It was concluded that  
178 denitrifiers dominated under carbon-limiting (i.e., high COD/N) conditions, whereas DNRA  
179 bacteria dominated under nitrate-limiting (i.e., high COD/N) conditions [3, 13]. Moreover, the  
180 coexistence of denitrifiers and DNRA bacteria was found for a wide range of intermediate  
181 influent COD/N ratios (Table S3).

182 Fig. 2 compares the measured and predicted competition outcomes at 12 conditions  
183 tested in the case studies. The predictions agreed with the measurements under 11 conditions  
184 tested (Fig. 2). The only condition (influent 5857 μM nitrate and 6278 μM acetate) where  
185 denitrification dominance was observed whereas coexistence was predicted (Fig. 2), was close  
186 to the predicted boundary, and microbial community analysis clearly evidenced the strong  
187 presence of DNRA bacteria at that point [3], implying that steady state may not have been  
188 reached yet experimentally at this point. Quantitatively, the predicted steady-state biomass  
189 concentrations and abundance were in good agreement with the measurements under all 7  
190 conditions tested in case study 1 (Fig. 3A and 3B, where influent resource concentrations  
191 were converted to COD/N ratio for simplicity). Overall, the predictions of this study were  
192 both qualitatively and quantitatively in close alignment with the measured data (Fig. 2 and 3).  
193 Therefore, the resource-ratio theory was considered valid for predicting the outcome of the  
194 competition between heterotrophic denitrifiers and DNRA bacteria in continuous systems.

195

196

### 197 **3.2 Impact of resource concentration on competition outcome**

198 The boundaries of the different regions in Fig. 2 can be expressed by the COD/N ratio, which  
199 is often used in literature for competition and field studies [3, 4, 10, 11]. Fig. 4 illustrates the  
200 influent COD/N ratios of the boundaries at different influent nitrate concentrations. These  
201 boundaries COD/N ratios define the tipping point at which one process prevails over or  
202 coexists next to the other. For instance, the upper boundary of the region for coexistence (i.e.,  
203 region 4) represented the minimum influent COD/N ratio for DNRA dominance, whereas its  
204 lower boundary represented the maximum influent COD/N ratio for DEN dominance (Fig. 4).  
205 Overall, the boundaries influent COD/N ratios changed significantly at low influent nitrate  
206 concentrations (e.g.,  $< 100 \mu\text{M}$ ) and gradually stabilized at high influent nitrate concentrations  
207 (e.g.,  $> 1000 \mu\text{M}$ ). With the increase of influent nitrate concentration, the region for  
208 coexistence (region 4) gradually widened and its upper and lower boundary influent COD/N  
209 ratios asymptotically approached the stoichiometric values of  $C_{\text{DNRA}}$  (corresponds to COD/N  
210 of 6.15) and  $C_{\text{DEN}}$  (corresponds to COD/N of 4.04), respectively. The stabilized boundaries at  
211 high influent nitrate concentration (Fig. 4) were also confirmed in Fig. 3B. Despite the large  
212 difference in influent nitrate concentration ( $1000 \mu\text{M}$  used for prediction vs.  $11790 \mu\text{M}$  in the  
213 experiments, Table S3), the predicted DNRA biomass fraction from the model agreed with the  
214 measurements (Fig. 3B). The trend also held for different influent COD concentrations (Fig.  
215 S4)

216 Overall, the results clearly illustrate that, as a governing factor of the competition  
217 between the two nitrate partitioning pathways, the boundary influent COD/N ratios were not  
218 constant but could change significantly with influent resource concentrations. At high  
219 influent resource concentrations, process stoichiometry (reflected in  $C_i$ ) of the two competing  
220 processes was the determining factor of the boundary influent COD/N ratios, whereas kinetics  
221 (i.e.,  $K_S$  and  $\mu_{\text{max}}$ , reflected in  $J_S$  and thus the ZNGIs, Fig. 2 & 4) were important as well but

222 only at low influent resource concentrations. This implies that influent COD/N ratio alone is  
223 not sufficient to predict the competition outcome of heterotrophic denitrification and DNRA.  
224 Different competition outcomes (resource limitation) could occur at the same influent COD/N  
225 ratio but varying influent resource concentrations (e.g., at the same influent COD/N ratio of  
226 6.86, all four possible competition outcomes could occur for points a, b, c, and d in Fig. 4,  
227 detailed Fig. S5). In this theoretical study, the competition between DEN and DNRA is  
228 determined by both stoichiometries and growth kinetics. The stoichiometries were assumed to  
229 be constant. The change of the boundary COD/N ratio with influent nitrate level was a result  
230 of the change of growth rate of two species and thus the contribution of the two processes at  
231 different influent nitrate concentrations.

232         The result also raises the question of how to anticipate the threshold of resource  
233 limitation in continuous cultures. Resource limitation is normally anticipated based on the  
234 process stoichiometry; for instance, nitrate is expected to be the limiting resource when it is  
235 lower than the stoichiometry would require in relation to COD [17]. Our results show that this  
236 stoichiometry-based definition is inadequate. For example, nitrate limitation (and thus DNRA  
237 dominance) would occur when the influent COD/N ratio was above 6.16 (close to the DNRA  
238 stoichiometry) at influent nitrate concentration of 1000  $\mu\text{M}$ , whereas it would only occur with  
239 the COD/N ratio above 8.05 at influent nitrate concentration of 10  $\mu\text{M}$  (Fig. 4).

240         The impact of resource concentrations on competition outcomes has significant  
241 implications, as different ecosystems have various nitrate availability (i.e., influent nitrate  
242 concentration) (Table 1) and therefore possibly different boundary COD/N ratios for nitrate  
243 partitioning. High nitrate concentrations have been reported in some ecosystems, for example,  
244 in groundwater at a nuclear waste site (up to 233mM [26]), in soil adjacent to bats guano  
245 caves [27], and in coastal rockpools affected by gull guano where high level of ammonium  
246 that can further result in high nitrate level due to nitrification was observed (e.g., 1600  $\mu\text{M}$

247 [28]). However, the nitrate concentrations in natural aquatic and terrestrial ecosystems are  
248 normally low (e.g.,  $<100 \mu\text{M}$ , Table 3), at which the boundaries of different competition  
249 outcomes changed dramatically (Fig. 4). Lab-scale competition studies often supply high  
250 concentrations of nitrate ( $> 1000 \mu\text{M}$ , e.g., in [3, 10, 16]) at which the boundaries were rather  
251 stable and mainly defined by the stoichiometries of denitrifiers and DNRA bacteria (Fig. 4).  
252 The thresholds obtained from these high-nitrate environments were closely resembled with  
253 our model. However, little experimental data is available for environmentally relevant  
254 scenarios with low nitrate conditions. It would be interesting to design experiments to check  
255 the theory under these conditions.

256 In the context of WWTPs, nitrate concentrations and COD/N ratios could change in a  
257 wide range along the treatment line. DNRA bacteria were shown to be enriched from  
258 activated sludge in chemostats with high COD/N ratio influent [3] and coexisted with  
259 denitrifiers in wastewater treatment wetlands [34, 35]. Besides, the use of biofilm reactors is  
260 increasing, where substrate gradients can be formed within the biofilm and may thus create  
261 microenvironments with high COD/N for DNRA to proliferate. The role of DNRA in  
262 WWTPs needs to be further characterized.

263 Some of the seemingly conflicting results concerning the impact of COD/N ratio may  
264 partially attribute to the type of system used for investigation, i.e., continuous (i.e., chemostat)  
265 versus batch cultures. In continuous cultures, the competition outcome is determined by the  
266 subsistence concentration for the limiting resource ( $J_s$ , Eq. 2), as shown in this study. Stable  
267 resource limitation can be reached in continuous cultures but not in batch cultures [13, 36]. In  
268 batch cultures, the competition outcome of different microorganisms is determined by their  
269 maximum growth rate [37]. Using both systems with a dual-pathway pure culture, Yoon et al.  
270 [10] suggested that the batch systems cannot resolve the impact of COD/N ratio on pathways  
271 selection between denitrification and DNRA. In a batch incubation system, the shift from

272 DEN to DNRA with increasing initial COD/N ratios, as expected in continuous cultures, was  
273 not established [14]. Fig. S6 demonstrates a straightforward comparison between these two  
274 systems. With the same initial conditions (COD/N ratio of 6.86, same of amount of DNRA  
275 and DEN bacteria), DNRA outcompeted DEN in a continuous culture at steady state with  
276 nitrate being the limiting substrate, whereas the opposite competition outcome was obtained  
277 in a batch culture (Fig. S6). Therefore, caution is required when comparing the results  
278 obtained from batch and continuous cultures.

### 279 **3.3 Impact of dilution rate on competition outcome**

280 In chemostats, the dilution rate (D) dictates the rate of resource supply and biomass washout.  
281 A species cannot survive in chemostats above a certain dilution rate (lower than its  $\mu_{max}$ ). The  
282 impact of D on single species has been well documented, for instance, in Kuenen and Johnson  
283 [38]. The impact of D on the coexistence of two species was therefore investigated closer.  
284 According to the resource-ratio theory, stable coexistence is only possible when denitrifiers  
285 and DNRA bacteria each have lower subsistence concentration for one of the two resources,  
286 i.e.,  $J_{NO_3}^{DEN} > J_{NO_3}^{DNRA}$  and  $J_{COD}^{DEN} < J_{COD}^{DNRA}$ . A critical dilution rate for coexistence ( $D_C =$   
287  $0.0435 \text{ h}^{-1}$ ) was thus calculated as a function of the  $\mu_{max}$  and  $K_S$  for nitrate of the two species  
288 (detailed in section S7). Below  $D_C$ , all four possible competition outcomes could occur,  
289 whereas above  $D_C$ , DNRA could not outcompete denitrification (Fig. 5A).

290 The boundaries of the region for coexistence (i.e., region 4 in Fig. 4) were used for  
291 illustrating the impact of investigated factors on competition outcomes since it is the  
292 conjunction region. Fig. 5B illustrates the impact of D on the boundaries of coexistence when  
293 D was lower than  $D_C$ . Firstly, with the increase of D, the  $J_s$  also increased (Eq. 2) and thus the  
294 minimum requirement for resources to sustain the biomass. Secondly, the impact of D was  
295 marginal at high influent nitrate concentrations (e.g.,  $>1000 \mu\text{M}$ ) but significant at low  
296 concentrations (Fig. 5B). At high influent concentrations, the upper and lower boundary

297 COD/N ratios were asymptotically approaching the stoichiometric values of  $C_{\text{DNRA}}$  and  $C_{\text{DEN}}$ ,  
298 respectively. At low influent concentrations, the impact became increasingly profound as D  
299 was approaching the critical dilution rate ( $D_C = 0.0435 \text{ h}^{-1}$ , Fig. 5B). For instance, the  
300 boundary COD/N ratios ( $\text{g COD g N}^{-1}$ ) for coexistence were 4.3-6.4 and 7.8-9.6 for a dilution  
301 rate of 0.026 and  $0.043 \text{ h}^{-1}$  (at influent nitrate concentration of  $100 \mu\text{M}$ , Fig. 5B), respectively.

302 Overall, the results highlight the importance of dilution rate on competition outcome,  
303 especially at low influent resource concentration and/or at high dilution rate. The critical  
304 dilution rate for coexistence ( $D_C$ ) enabled to justify the measured competition outcomes by  
305 Rehr and Klemme, (1989). In mixed pure cultures of DNRA bacteria (*Citrobacter freundii*)  
306 and denitrifiers (*Pseudomonas stutzeri*) competing for nitrate and lactate, stable coexistence  
307 was obtained at low dilution rate ( $0.05 \text{ h}^{-1}$ ) whereas DNRA bacterium started to be washed  
308 out at a dilution rate ( $0.1 \text{ h}^{-1}$ ) much lower than its  $\mu_{\text{max}}$  ( $0.19 \text{ h}^{-1}$ ) [16]. The results on the  
309 impact of dilution rate were in agreement with the observations in environmental enrichments  
310 by Kraft et al. [11] where denitrifiers outcompeted DNRA bacteria at lower generation time  
311 (thus higher dilution rate) even under nitrate-limiting conditions. Regarding the COD/N range  
312 for coexistence, van den Berg et al. [13] suggested that it should be independent of the  
313 dilution rate. Apparently, this only holds at high resource concentrations (as used in their  
314 study) but not at low resource concentrations (e.g.,  $< 1000 \mu\text{M}$ , Fig. 5B). In a similar  
315 competition scenario, Tilman [39] studied the impact of the ratio of two nutrients on the  
316 competition outcomes of two algae species and found an apparent curvature of the boundary  
317 between stable coexistence and one species dominance at high flow rate (i.e., dilution rate),  
318 confirming the impact shown in Fig. 5B.

### 319 **3.4 Impact of kinetic and stoichiometric parameters on competition outcome**

320 A sensitivity analysis was conducted to investigate the impact of kinetic and stoichiometric  
321 parameters (i.e.,  $K_s$ ,  $\mu_{max}$ , and  $Y$ ) on the competition outcome (Fig. 6). The default values of  
322 these parameters (Table S2) were used for the reference case. These parameters are species-  
323 specific and may change between different denitrifiers and DNRA bacteria. The fate of nitrate  
324 is therefore subject to the local communities in an (micro-) ecosystem. The parameters for the  
325 same bacteria may also be affected by the environmental conditions (e.g., temperature and  
326 pH). For instance, the  $\mu_{max}$  increases with temperature within a certain temperature range.  
327 Consequently, the difference between the  $\mu_{max}$  of DNRA and DEN may also increase due to  
328 global warming and thus affect the fate of nitrate. The sensitivity analysis has the power to  
329 unravel the trend in response to the variation of the parameters and can thus give insight into  
330 their potential impact on the competition outcome.

#### 331 **3.4.1 Affinity constants for the resources**

332 The ratio of the affinity constants of the two species for nitrate/COD was changed in two  
333 magnitudes (Fig. 6A). Stable coexistence (i.e.,  $0 < \text{fraction of DNRA} < 1$ ) was only possible  
334 when the ratio of the affinity constant for nitrate (i.e.,  $K_{NO_3}^{DNRA} / K_{NO_3}^{DEN}$ ) was lower than  
335 0.43 (Fig. 6A, section S8), indicating that a sufficiently higher affinity of DNRA for nitrate  
336 relative to DEN is required. In contrast, the ratio of the affinity constant for COD (i.e.,  
337  $K_{COD}^{DNRA} / K_{COD}^{DEN}$ ) had to be higher than 0.43 for coexistence (Fig. 6A, section S8). This  
338 threshold (i.e., 0.43) was determined by the  $\mu_{max}$  of the two species and the  $D$  of the  
339 continuous culture (detailed in section S8). Regarding the absolute values of affinity constants,  
340 with the simultaneous increase of  $K_{NO_3}^{DNRA}$  and  $K_{NO_3}^{DEN}$  (at fixed  $K_{NO_3}^{DNRA} / K_{NO_3}^{DEN}$  ratio),  
341 the pattern changed from DNRA-favored (reference case) to coexistence-favored and further  
342 to DEN-favored pattern (Fig. 6B). This implies that the lower the affinity for nitrate of the



343 two competing species, the lower the threshold (minimum COD/N ratio) for DNRA  
344 dominance, especially at low nitrate concentration.

345 Affinity for the competing resources is often used to predict competition outcomes [40,  
346 41]. The result demonstrated that the species with higher affinity (i.e., lower  $K_s$ ) for the  
347 limiting resources did not necessarily outcompete other species in continuous cultures (e.g.,  
348 when  $K_{NO_3}^{DNRA} / K_{NO_3}^{DEN} = 0.2$  and  $K_{COD}^{DNRA} / K_{COD}^{DEN} = 0.5$ , DNRA bacteria would have a  
349 higher affinity for both nitrate and COD. Nevertheless, stable coexistence rather than the  
350 displacement of DEN was possible (Fig. 6A)). This illustrates that affinity alone was not  
351 sufficient to predict the competition outcome in continuous cultures. The  $\mu_{max}$  and  $D$  need to  
352 be taken into account as well, as expressed by  $J_s$  parameter (Eq. 2) [19, 21, 42].

### 353 3.4.2 Maximum specific growth rate

354 The difference between the  $\mu_{max}$  of the two species (i.e.,  $\Delta\mu_{max} = \mu_{max}^{DEN} - \mu_{max}^{DNRA}$ ) was used for  
355 sensitivity analysis (Fig. 6C). The increase of  $\Delta\mu_{max}$  led to no pattern change but a higher  
356 threshold for coexistence, whereas the decrease of  $\Delta\mu_{max}$  resulted in a gradual shift towards  
357 the coexistence-favored pattern. This implies that the bigger the difference between the  $\mu_{max}$   
358 of the two competing species, the more likely the dominance of denitrification at low resource  
359 concentrations would be (i.e., the higher the maximum COD/N ratio for DEN dominance).  
360 The constraint for  $\mu_{max}$  to allow stable coexistence was detailed in section S8.

### 361 3.4.3 Yield coefficient

362 Regarding the yield coefficient, the  $C$  criterion (i.e., the ratio of  $Y_{NO_3}$  to  $Y_{COD}$ , Eq. 4) of the two  
363 competing species was used for sensitivity analysis (Fig. 6D). Results show that it only  
364 affected the upper or lower limits. The higher the difference between  $C_{DNRA}$  and  $C_{DEN}$  (i.e.,  
365 higher  $\Delta C$ ), the broader the region for coexistence (Fig. 6D). This was in line with the  
366 observations of the two case studies used for theory verification (Table S3). A lower  $\Delta C$  was  
367 measured in case 2 [3] relative to case 1 [13] and thereby a narrowed region for coexistence in

368 case 2. Noteworthy, if  $C_{\text{DNRA}}$  were lower than  $C_{\text{DEN}}$ , stable coexistence would no longer be  
369 possible [18, 19], which in turn supported the measured higher biomass yield over nitrate of  
370 DNRA bacteria than that of denitrifiers [3, 9].

#### 371 **3.4.4 Overall impact of kinetic and stoichiometric parameters**

372 The sensitivity analysis illustrated that kinetic and stoichiometric parameters (i.e.,  $K_s$ ,  $\mu_{\text{max}}$ ,  
373 and  $Y$ ) affected both the possibility and the boundaries of stable coexistence of denitrifiers and  
374 DNRA bacteria. In the region for stable coexistence,  $K_s$  and  $\mu_{\text{max}}$  of the two competing  
375 species had a significant impact on the boundaries and thus the competition outcome mainly  
376 at low resources concentrations (e.g.,  $<100 \mu\text{M}$  nitrate). The yield coefficients (reflected on  $C_i$ )  
377 could shift the boundaries across all concentration spectra and had a greater impact at high  
378 concentrations than at low influent concentrations.

#### 379 **3.5 Dynamic system behaviour**

380 Fig. 7 demonstrates the trajectories to stable coexistence at steady state, with the evolution of  
381 the two competing species and two resources in Fig. 7A and the calculated growth rates ( $\mu$ ,  
382 Eq.1&3) in Fig. 7B. In the dynamic system behaviour, four phases could be distinguished  
383 based on the limiting resource for the growth of DNRA(Fig. 7B).

384 In phase I, the growth of DNRA was limited by acetate ( $\mu_{\text{DNRA}}=\mu_{\text{DNRA,C}}$ , Fig. 7B). The  
385 concentration of nitrate and acetate in the chemostat decreased with the growth of denitrifiers  
386 and DNRA bacteria (Fig. 7A), which in turn resulted in their decreased growth rates (Fig. 7B).  
387 By the end of phase I, nitrate concentration reached  $J_{\text{NO}_3}^{\text{DNRA}} (< J_{\text{NO}_3}^{\text{DEN}})$ , at which the growth  
388 rate of denitrifiers ( $\mu_{\text{DEN}}$ ) could not balance the loss rate ( $\mu_{\text{DEN}}<D$ , Fig. 7B) and the biomass  
389 concentration of denitrifiers thus decreased (Fig. 7A). In phase II, the growth of DNRA was  
390 limited by nitrate ( $\mu_{\text{DNRA}}=\mu_{\text{DNRA,N}}$ , Fig. 7B) and the low nitrate concentration favored DNRA  
391 bacteria, i.e.,  $\mu_{\text{DNRA}}>\mu_{\text{DEN}}$  (Fig. 7B). Meanwhile, acetate concentration decreased further and  
392 reached a point where the growth of DNRA bacteria shifted to become acetate-limited again

393 ( $\mu_{\text{DNRA}} = \mu_{\text{DNRA,C}}$ , phase III, Fig. 7B). In phase III,  $\mu_{\text{DNRA}}$  started decreasing with decreasing  
394 acetate concentration, resulting in a lower nitrate consumption by DNRA bacteria.  
395 Consequently, the nitrate concentration gradually recovered to reach  $J_{\text{NO}_3}^{\text{DEN}}$ . Simultaneously,  
396 the acetate concentration further decreased to reach  $J_{\text{COD}}^{\text{DNRA}} (> J_{\text{NO}_3}^{\text{DEN}})$  by the end of phase  
397 III. From this point, the growth rate of the two competing species became identical and  
398 equaled to dilution rate of the chemostat and thereby reached the steady state (phase IV).

399 Noteworthy, both nitrate and acetate were limiting (i.e., dual limitation) in phase  
400 III&IV, with DNRA being acetate-limited ( $J_{\text{COD}}^{\text{DNRA}} > J_{\text{COD}}^{\text{DEN}}$ ) and DEN nitrate-limited  
401 ( $J_{\text{NO}_3}^{\text{DEN}} > J_{\text{NO}_3}^{\text{DNRA}}$ ). Therefore, coexistence occurred at steady state because each species  
402 was limited by the resource for which its rival has the lower subsistence concentration ( $J_S$ )  
403 and thus competitive advantage, i.e., DNRA by acetate whereas DEN by nitrate. This is in  
404 line with the proposed theoretical condition for coexistence [18, 19, 43] and observed  
405 competition behavior (i.e., dual-limitation of acetate and nitrate at stable coexistence [13]).

### 406 **3.6 Model assumptions and their implications**

407 In this study, denitrification and DNRA were assumed to directly compete for nitrate and be  
408 carried out by two distinct specialist species. This section discusses the role of nitrite, the  
409 potential difference between specialist and dual-pathway species and the complexity of  
410 electron donor (organics), and their implications in predicting the competition outcome.

411 Nitrite is the common intermediate and the branching point of the two pathways, and  
412 both nitrate and nitrite can be the terminal electron acceptors in DEN and DNRA [1].  
413 However, there is still a lack of consensus about the role of nitrite in their competition. Kraft  
414 et al. [11] found a shift from DNRA to DEN when nitrate was replaced by nitrite in chemostat  
415 enrichment systems with marine sediments and postulated nitrite as a determining factor in  
416 the selection of the two pathways, suggesting that denitrifiers have a comparatively higher

417 affinity for nitrite. Yoon et al. [44] showed the ratio of nitrite to nitrate was determinative in  
418 pathway selection in a chemostat study with dual-pathway pure culture, with DNRA  
419 dominated at higher nitrite/nitrate ratios. In contrast, van den Berg et al. [45] demonstrated  
420 that nitrite does not generally control the competition between denitrification and DNRA in  
421 chemostat enrichment cultures. In general, if there is nitrite accumulation, there is no need to  
422 consider nitrite in the model. If the competition of denitrification and DNRA only lies in the  
423 nitrite reduction, then the resource-ratio theory could be easily implemented in the same way.  
424 However, the parameters related to nitrite (e.g.,  $K_s$  and yield) are still largely missing and  
425 need further determination. In case where nitrite accumulation is observed, the applicability of  
426 the resource-ratio theory would be limited as it would not be suitable to describe DEN and  
427 DNRA as one-step reactions.

428         The possible difference between dual-pathway and specialist microorganisms deserves  
429 further clarification. In dual-pathway microorganisms, the first step (i.e., nitrate reduction to  
430 nitrite) may be catalyzed by the same enzyme, and the competition of the two pathways  
431 would thus lie on nitrite. For example, the dual-pathway *Shewanella loihica* PV-4 utilizes  
432 NapA and *I. calvum* utilizes NarG for nitrate reduction [17]. This may explain the observed  
433 determining effect of nitrite on pathway selection in *Shewanella loihica* PV-4 [44] but not in  
434 the enrichment cultures where different bacteria are responsible for denitrification and DNRA  
435 [45]. Moreover, the competition between two species could result in the displacement of the  
436 rival, whereas competition of two pathways within the same microorganism may depend on  
437 the maximum benefit (e.g., maximum energy production or electron transfer) for the  
438 microorganism under certain conditions.

439         The results in this study revealed what determined the boundary COD/N ratios of  
440 different competition outcomes between heterotrophic DEN and DNRA, using a non-  
441 fermentative acetate as an example for electron donors (i.e., organics). However, the nature of

442 organics can be complex and have been shown to affect the competition outcome [11, 16, 46].  
443 The presence of fermentative organic carbon (e.g., lactate) may stimulate fermentative  
444 bacteria which can directly compete for both nitrate and organic carbon through fermentative  
445 DNRA process [47] and/or alter the organic carbon available for denitrifiers and DNRA  
446 bacteria [46]. Consequently, a higher influent COD/N ratio may be needed for DNRA  
447 dominance [46]. Previous study suggested that the nitrogen conversions in the oxygen  
448 minimum zones (OMZs) of the ocean was likely regulated by organic carbon [29]. The  
449 composition and concentration of organic carbon can change both spatially and temporally  
450 and different organic compounds may have different influence on various microbial processes  
451 [29, 48, 49]. More detailed organic geochemical analyses in different ecosystems and  
452 incorporation of fermentative bacteria in the DNRA modeling are of interest for future studies.

### 453 **3.7 Potential further applications of the resource-ratio theory**

454 One commonly accepted theory for interspecies competition for the same substrate is the K/r  
455 strategist hypothesis [50, 51]. With the default kinetics currently available, DNRA resembles  
456 a K-strategist (species with high substrate affinity and low  $\mu_{max}$ ) and DEN a r-strategist  
457 (species with low substrate affinity and high  $\mu_{max}$ ). According to this theory, DNRA would  
458 win the competition against DEN when both organisms are subjected to low-nitrate conditions  
459 (i.e., high COD/N), which agrees with the prediction of the resource-ratio theory that was  
460 used here (Fig. 4) and that are also confirmed experimentally [3, 16]. Nevertheless, the K/r  
461 strategist hypothesis only considers one limiting substrate (nitrate or COD), whereas the  
462 resource-ratio theory simultaneously takes both limiting substrates (and dilution rate) into  
463 account and is thus more comprehensive.

464 In this study, the resource-ratio theory was applied to elucidate the competition  
465 between denitrification and DNRA for nitrate and organic carbon. Nevertheless, the  
466 conclusions and their implications can be extended to other similar competition scenarios, for

467 instance, the competition between ammonia-oxidizing bacteria (AOB), archaea (AOA) and  
468 comammox microorganisms for ammonia and oxygen, and the competition between sulfide-  
469 based autotrophic denitrification and DNRA. As demonstrated in this study and previously  
470 [52–54], the resource ratio-theory offers mechanistic insights and quantitative prediction of  
471 competition outcomes between microorganisms for common resources. Despite its relatively  
472 easy implementation and great value, its application in the microbial competition is still rather  
473 limited. To ease the application, a decision tree (Fig. S2) and a spreadsheet model  
474 (Supplementary Information\_2) were created and provided for the generalized scenario where  
475 two species exploitatively compete for two essential resources, as is the case for DEN and  
476 DNRA.

#### 477 **4. Conclusions**

478 The resource-ratio theory was applied to elucidate the competition between heterotrophic  
479 denitrification and DNRA in continuous cultures and verified with experimental results. The  
480 results highlight the impact of resource concentrations, dilution rate and microbial kinetic and  
481 stoichiometric parameters on the boundary COD/N ratios and thus the competition outcome.  
482 The COD/N ratio dictated the competition between the two nitrate partitioning pathways,  
483 however, the boundary values changed significantly with influent resource concentrations. At  
484 high influent resource concentrations, the stoichiometries (i.e., consumption of COD per  
485 nitrate) of the two competing processes was the determining factor of the boundary COD/N  
486 ratios, whereas kinetics (i.e.,  $K_S$  and  $\mu_{max}$ ) was important as well but only at low influent  
487 resource concentrations. The dilution rate became significant at low influent resource  
488 concentration and/or high values close to the critical ones. At stable coexistence, the growth  
489 of DNRA and DEN was limited by COD and nitrate, respectively. The results also provide  
490 testable hypotheses concerning the nitrate partitioning at environmentally relevant low nitrate

491 conditions for further research. The conclusions based on the verified resource-ratio theory  
492 potentially have broad implications for similar competition scenarios.

### 493 **Conflict of Interest**

494 The authors declare no conflicts of interest.

### 495 **Acknowledgments**

496 Mingsheng Jia acknowledges the support from China Scholarship Council (CSC) and the  
497 special research fund (BOF) from Ghent University. The authors acknowledge Dana Ofiteru,  
498 Diederik Rousseau, Mathieu Sperandio, Michele Laurenzi, Jose Maria Carvajal Arroyo, and  
499 Nico Boon for their constructive discussions on this work.

500

## 501 **References**

- 502 1. Kraft B, Strous M, Tegetmeyer HE. Microbial nitrate respiration - Genes, enzymes and  
503 environmental distribution. *J Biotechnol* 2011; **155**: 104–117.
- 504 2. Canfield DE, Glazer AN, Falkowski PG. The evolution and future of earth's nitrogen  
505 cycle. *Science (80- )*. 2010. American Association for the Advancement of Science. ,  
506 **330**: 192–196
- 507 3. Van Den Berg EM, Van Dongen U, Abbas B, Van Loosdrecht MCM. Enrichment of  
508 DNRA bacteria in a continuous culture. *ISME J* 2015; **9**: 2153–2161.
- 509 4. Rütting T, Boeckx P, Müller C, Klemmedtsson L. Assessment of the importance of  
510 dissimilatory nitrate reduction to ammonium for the terrestrial nitrogen cycle.  
511 *Biogeosciences* 2011; **8**: 1779–1791.
- 512 5. Giblin AE, Tobias CR, Song B, Weston N, Banta GT, Rivera-Monroy VH. The  
513 importance of dissimilatory nitrate reduction to ammonium (DNRA) in the nitrogen  
514 cycle of coastal ecosystems. *Oceanography* 2013; **26**: 124–131.
- 515 6. Burgin AJ, Hamilton SK. Have we overemphasized the role of denitrification in  
516 aquatic ecosystems? A review of nitrate removal pathways. *Front Ecol Environ* . 2007. ,  
517 **5**: 89–96
- 518 7. Kuypers MMM, Marchant HK, Kartal B. The microbial nitrogen-cycling network.  
519 *Nature Reviews Microbiology* . 2018.
- 520 8. Tiedje JM. Ecology of denitrification and dissimilatory nitrate reduction to ammonium.  
521 In: Zehnder AJB (ed). *Environmental Microbiology of Anaerobes*. 1988. John Wiley  
522 Sons, New York, pp 179–244.
- 523 9. Strohm TO, Griffin B, Zumft WG, Schink B. Growth yields in bacterial denitrification  
524 and nitrate ammonification. *Appl Environ Microbiol* 2007; **73**: 1420–1424.
- 525 10. Yoon S, Cruz-García C, Sanford R, Ritalahti KM, Löffler FE. Denitrification versus  
526 respiratory ammonification: Environmental controls of two competing dissimilatory  
527 NO<sub>3</sub><sup>-</sup>/NO<sub>2</sub><sup>-</sup>-reduction pathways in *Shewanella loihica* strain PV-4. *ISME J* 2015; **9**:  
528 1093–1104.
- 529 11. Kraft B, Tegetmeyer HE, Sharma R, Klotz MG, Ferdelman TG, Hettich RL, et al. The  
530 environmental controls that govern the end product of bacterial nitrate respiration.  
531 *Science (80- )* 2014; **345**: 676–679.
- 532 12. Tiedje JM. Ecology of denitrification and dissimilatory nitrate reduction to ammonium.  
533 *Environ Microbiol Anaerobes* 1988; 179–244.
- 534 13. van den Berg EM, Boleij M, Kuenen JG, Kleerebezem R, van Loosdrecht MCM.  
535 DNRA and denitrification coexist over a broad range of acetate/N-NO<sub>3</sub><sup>-</sup> ratios, in a  
536 chemostat enrichment culture. *Front Microbiol* 2016; **7**: 1–12.
- 537 14. Behrendt A, Tarre S, Beliaevski M, Green M, Klatt J, de Beer D, et al. Effect of high  
538 electron donor supply on dissimilatory nitrate reduction pathways in a bioreactor for  
539 nitrate removal. *Bioresour Technol* 2014; **171**: 291–297.



- 540 15. Sotta ED, Corre MD, Veldkamp E. Differing N status and N retention processes of  
541 soils under old-growth lowland forest in Eastern Amazonia, Caxiuanã, Brazil. *Soil Biol*  
542 *Biochem* 2008; **40**: 740–750.
- 543 16. Rehr B, Klemme JH. Competition for nitrate between denitrifying *Pseudomonas*  
544 *stutzeri* and nitrate ammonifying enterobacteria. *FEMS Microbiol Lett* 1989; **62**: 51–57.
- 545 17. Vuono DC, Read RW, Hemp J, Sullivan BW, Arnone JA, Neveux I, et al. Resource  
546 concentration modulates the fate of dissimilated nitrogen in a dual-pathway  
547 actinobacterium. *Front Microbiol* 2019; **10**: 3.
- 548 18. Tilman D. Resources: A Graphical-Mechanistic Approach to Competition and  
549 Predation. *Am Nat* 1980; **116**: 362–393.
- 550 19. Hsu S-B, Cheng K-S, Hubbell SP. Exploitative Competition of Microorganisms for  
551 Two Complementary Nutrients in Continuous Cultures. *SIAM J Appl Math* 1981; **41**:  
552 422–444.
- 553 20. Williamson M, MacArthur RH. Geographical Ecology. Patterns in the Distribution of  
554 Species. *J Anim Ecol* 1974; **43**: 601.
- 555 21. Hansen SR, Hubbell SP. Single-nutrient microbial competition: Qualitative agreement  
556 between experimental and theoretically forecast outcomes. *Science (80- )* 1980; **207**:  
557 1491–1493.
- 558 22. Tilman D. Ecological Competition Between Algae □: Experimental Confirmation of  
559 Resource-Based Competition Theory. *Science (80- )* 1976; **192**: 463–465.
- 560 23. Volcke EIP, Loccufier M, Vanrolleghem PA, Noldus E JL. Existence, uniqueness and  
561 stability of the equilibrium points of a SHARON bioreactor model. *J Process Control*  
562 2006; **16**: 1003–1012.
- 563 24. Monod J. La technique de culture continue: theorie et applications. *Ann Inst Pasteur*  
564 1950; 390–410.
- 565 25. Hsu SB, Hubbell S, Waltman P. A Mathematical Theory for Single-Nutrient  
566 Competition in Continuous Cultures of Micro-Organisms. *SIAM J Appl Math* 1977; **32**:  
567 366–383.
- 568 26. Fortney JL, Mehlhorn TL, Lowe KA, Earles JE, Phillips J, Techtmann SM, et al.  
569 Natural Bacterial Communities Serve as Quantitative Geochemical Biosensors. *MBio*  
570 2015; **6**: 1–13.
- 571 27. Pellegrini TG, Ferreira RL. Structure and interactions in a cave guano-soil continuum  
572 community. *Eur J Soil Biol* 2013; **57**: 19–26.
- 573 28. Loder TC, Ganning B, Love JA. Ammonia nitrogen dynamics in coastal rockpools  
574 affected by gull guano. *J Exp Mar Bio Ecol* 1996; **196**: 113–129.
- 575 29. Lam P, Kuypers MMM. Microbial Nitrogen Cycling Processes in Oxygen Minimum  
576 Zones. *Ann Rev Mar Sci* 2011; **3**: 317–345.
- 577 30. Spalding RF, Exner ME. Occurrence of nitrate in groundwater - A review. *J Environ*  
578 *Qual* 1993; **22**: 392–402.

- 579 31. EC. Report on the implementation of Council Directive 91/676/EEC concerning the  
580 protection of waters against pollution caused by nitrates from agricultural sources  
581 based on Member State reports for the period 2012-2015. 2018.
- 582 32. Bonin P. Anaerobic nitrate reduction to ammonium in two strains isolated from coastal  
583 marine sediment: A dissimilatory pathway. *FEMS Microbiol Ecol* 1996; **19**: 27–38.
- 584 33. Henze M, van Loosdrecht MCM, Ekama GA, Brdjanovic D. Biological Wastewater  
585 Treatment: Principles, Modelling and Design. *Water Intelligence Online* . 2008. IWA  
586 Pub.
- 587 34. Jahangir MMR, Fenton O, Müller C, Harrington R, Johnston P, Richards KG. In situ  
588 denitrification and DNRA rates in groundwater beneath an integrated constructed  
589 wetland. *Water Res* 2017; **111**: 254–264.
- 590 35. Rahman MM, Roberts KL, Grace MR, Kessler AJ, Cook PLM. Role of organic carbon,  
591 nitrate and ferrous iron on the partitioning between denitrification and DNRA in  
592 constructed stormwater urban wetlands. *Sci Total Environ* 2019; **666**: 608–617.
- 593 36. Kuenen JG, Johnson OJ. Continuous Cultures (Chemostats). *Encyclopedia of*  
594 *Microbiology* . 2009. Elsevier Inc.
- 595 37. Veldkamp H, Kuenen JG. The Chemostat as a Model System for Ecological Studies.  
596 *Bull Ecol Res Comm* 1973; **17**: 347–355.
- 597 38. Kuenen JG, Johnson OJ. Continuous Cultures (Chemostats). *Encyclopedia of*  
598 *Microbiology*. 2009. Elsevier, pp 130–147.
- 599 39. Tilman D. Resource Competition between Plankton Algae: An Experimental and  
600 Theoretical Approach. *Ecology* 1977; **58**: 338–348.
- 601 40. Dimitri Kits K, Sedlacek CJ, Lebedeva E V., Han P, Bulaev A, Pjevac P, et al. Kinetic  
602 analysis of a complete nitrifier reveals an oligotrophic lifestyle. *Nature* 2017; **549**:  
603 269–272.
- 604 41. Straka LL, Meinhardt KA, Bollmann A, Stahl DA, Winkler MKH. Affinity informs  
605 environmental cooperation between ammonia-oxidizing archaea (AOA) and anaerobic  
606 ammonia-oxidizing (Anammox) bacteria. *ISME J* 2019.
- 607 42. Winkler MKH, Boets P, Hahne B, Goethals P, Volcke EIP. Effect of the dilution rate  
608 on microbial competition: R-strategist can win over kstrategist at low substrate  
609 concentration. *PLoS One* 2017; **12**: e0172785.
- 610 43. Bader FG. Analysis of double□substrate limited growth. *Biotechnol Bioeng* 1978; **20**:  
611 183–202.
- 612 44. Yoon S, Sanford RA, Löffler FE. Nitrite control over dissimilatory nitrate/nitrite  
613 reduction pathways in *Shewanella loihica* strain PV-4. *Appl Environ Microbiol* 2015;  
614 **81**: 3510–3517.
- 615 45. van den Berg EM, Rombouts JL, Kuenen JG, Kleerebezem R, van Loosdrecht MCM.  
616 Role of nitrite in the competition between denitrification and DNRA in a chemostat  
617 enrichment culture. *AMB Express* 2017; **7**: 91.

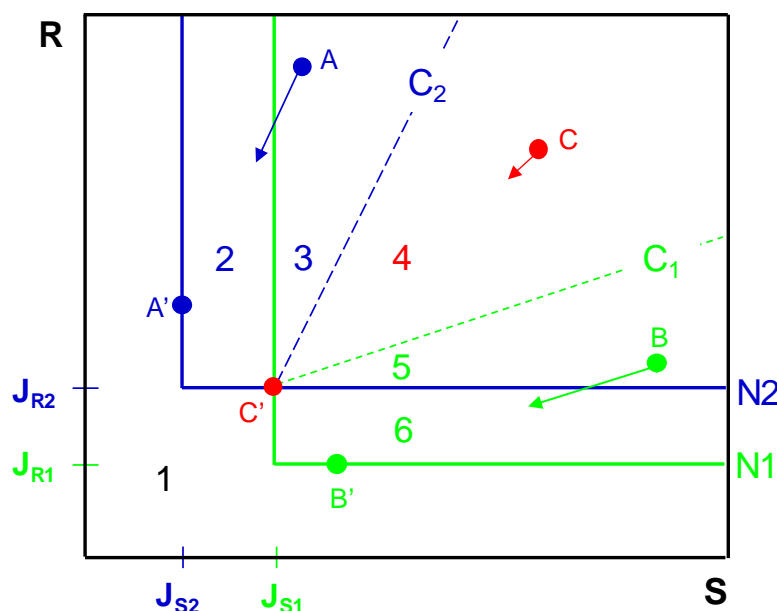
- 618 46. van den Berg EM, Elisário MP, Kuenen JG, Kleerebezem R, van Loosdrecht MCM.  
619 Fermentative bacteria influence the competition between denitrifiers and DNRA  
620 bacteria. *Front Microbiol* 2017; **8**: 1684.
- 621 47. Cole J. Nitrate reduction to ammonia by enteric bacteria: Redundancy, or a strategy for  
622 survival during oxygen starvation? *FEMS Microbiol Lett* . 1996. Narnia. , **136**: 1–11
- 623 48. Muscarella ME, Boot CM, Broeckling CD, Lennon JT. Resource heterogeneity  
624 structures aquatic bacterial communities. *ISME J* 2019; 1.
- 625 49. Kovárová-Kovar K, Egli T. Growth kinetics of suspended microbial cells: from single-  
626 substrate-controlled growth to mixed-substrate kinetics. *Microbiol Mol Biol Rev* 1998;  
627 **62**: 646–66.
- 628 50. Dorodnikov M, Blagodatskaya E, Blagodatsky S, Fangmeier A, Kuzyakov Y.  
629 Stimulation of r- vs. K-selected microorganisms by elevated atmospheric CO<sub>2</sub> depends  
630 on soil aggregate size: Research article. *FEMS Microbiol Ecol* 2009; **69**: 43–52.
- 631 51. Andrews JH, Harris RF. r- and K-Selection and Microbial Ecology. 1986. Springer,  
632 Boston, MA, pp 99–147.
- 633 52. Smith VH, Graham DW, Cleland DD. Application of resource-ratio theory to  
634 hydrocarbon biodegradation. *Environ Sci Technol* 1998; **32**: 3386–3395.
- 635 53. Miller TE, Burns JH, Munguia P, Walters EL, Kneitel JM, Richards PM, et al. A  
636 critical review of twenty years' use of the resource-ratio theory. *Am Nat* 2005; **165**:  
637 439–448.
- 638 54. Bellucci M, Ofițeru ID, Beneduce L, Graham DW, Head IM, Curtis TP. A preliminary  
639 and qualitative study of resource ratio theory to nitrifying lab-scale bioreactors. *Microb*  
640 *Biotechnol* 2015; **8**: 590–603.

641

642

643

644

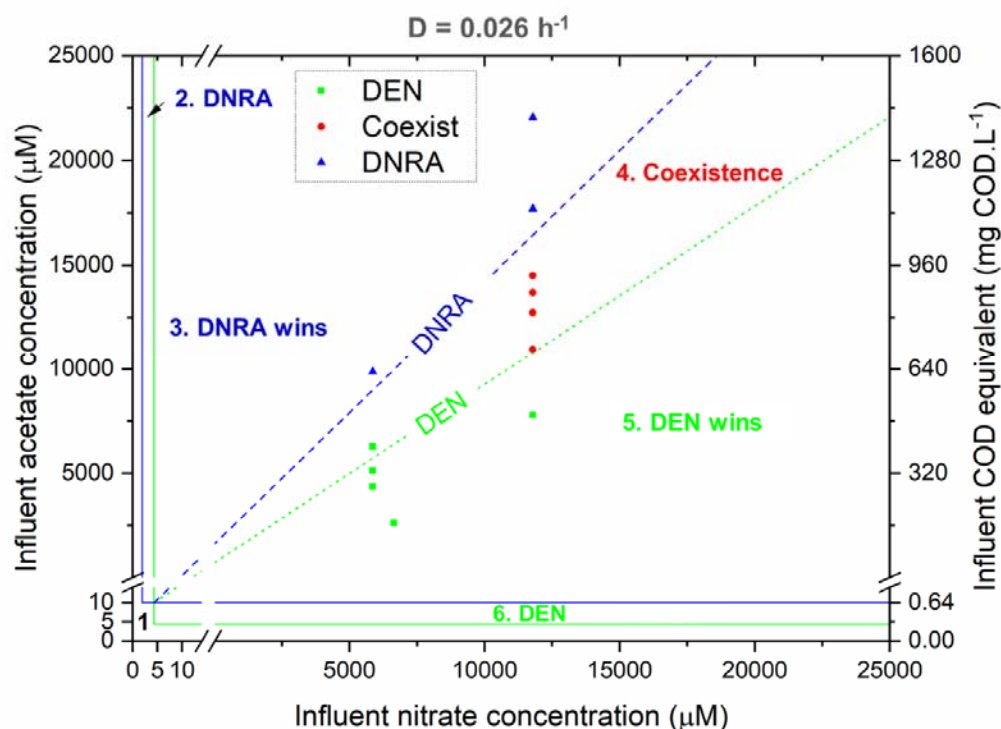


645

646 **Figure 1.** Graphical representation of resource competition of two species (N1 and N2) competing for  
 647 two resources (S and R) at a specific dilution rate. The solid lines labeled N1 and N2 are the Zero Net  
 648 Growth Isoclines (ZNGIs) for the two species. The dashed lines are the consumption vectors for the  
 649 two species, with the slope of C1 and C2, respectively. The competition outcomes can be predicted  
 650 from the supply point (defined by the supplied concentration of resource S and R in this S-R plane,  
 651 e.g., points A, B and C). Region 1, no species can survive; Region 2, only species N2 can survive;  
 652 Region 3, species N2 outcompetes species N1, dynamic behavior (trajectory) governed by slope C<sub>2</sub>;  
 653 Region 4, the two species stably coexist; Region 5, species N1 outcompetes species N2, dynamic  
 654 behavior (trajectory) governed by slope C<sub>1</sub>; Region 6, only species N1 can survive. The equilibrium  
 655 points always fall on the ZNGIs. Points A', B' and C' represent the corresponding equilibrium points  
 656 of supply points A, B and C. Line A-A' has the same slope as C<sub>2</sub>, whereas line B-B' has the same  
 657 slope of C<sub>1</sub>. All supply points in region 4 would reach the same equilibrium point C'.

658

659

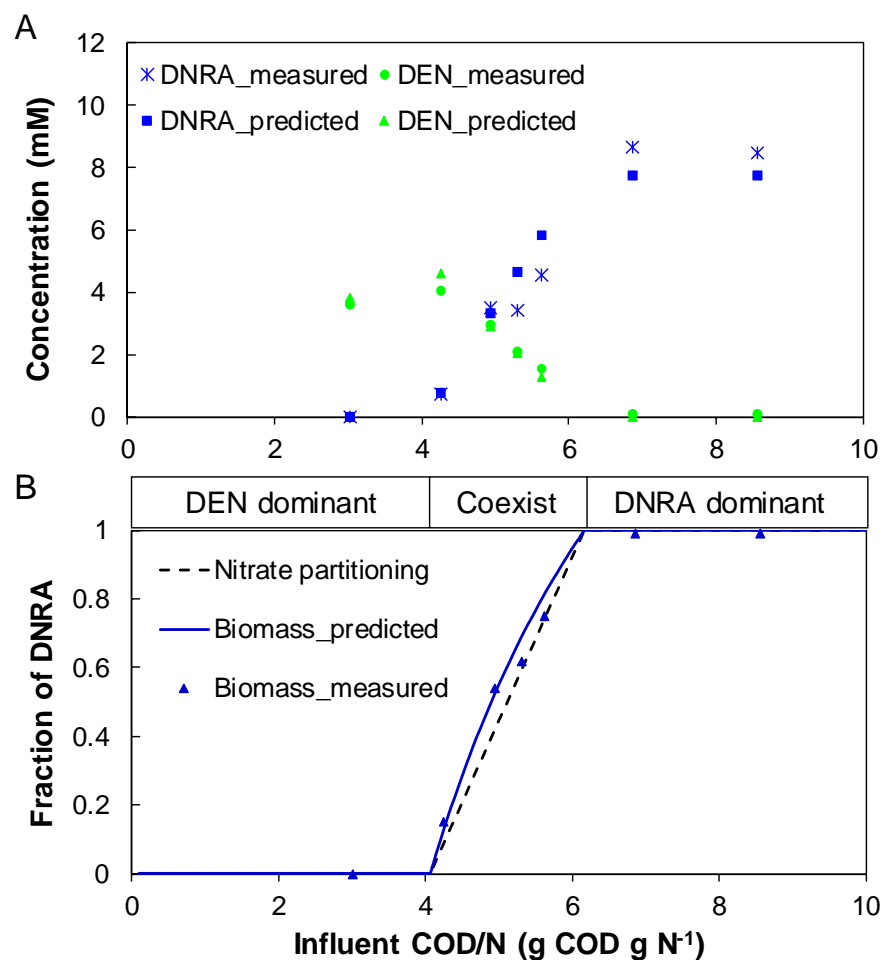


660

661 **Figure 2.** Predicted and observed outcomes of competition for nitrate and organic carbon by  
662 heterotrophic denitrifiers and DNRA bacteria in continuous cultures at a dilution rate of  $0.026 \text{ h}^{-1}$ .  
663 Experiments [3, 13] for which DEN was dominant are shown with green squares; those for which  
664 DNRA was dominant are shown with blue triangles, and those for which coexistence was observed are  
665 shown with red dots. The borders and the meaning of the operating zones distinguished by the  
666 resource-ratio theory are detailed in Figure 1. The consumption vectors (broken lines) have a slope of  
667  $C_{\text{DEN}} (4.04 \text{ g COD g N}^{-1})$  for denitrifiers and  $C_{\text{DNRA}} (6.15 \text{ g COD g N}^{-1})$  for DNRA bacteria.

668

669

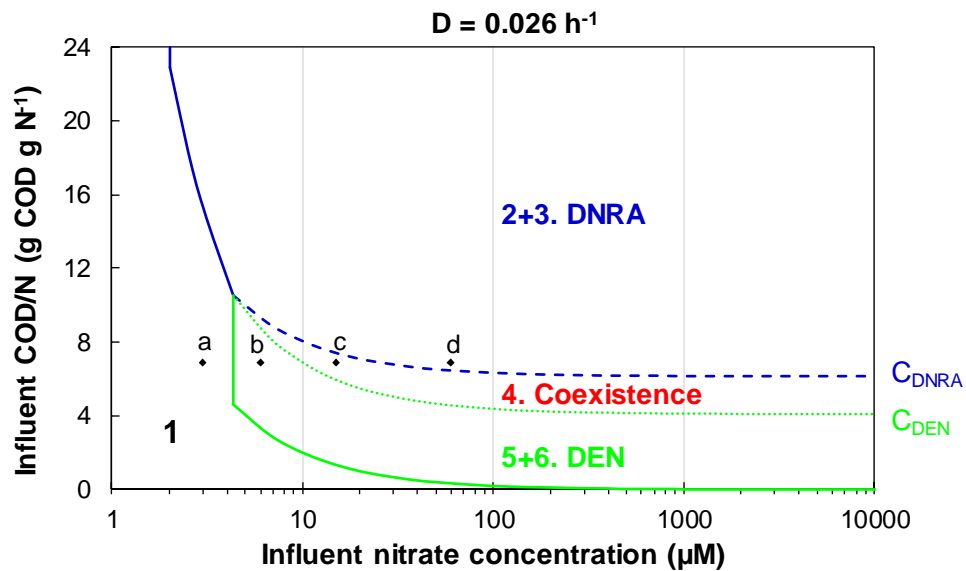


670

671 **Figure 3.** Prediction versus measurement at steady state (case study 1 [13]): (A) concentrations of  
672 heterotrophic denitrifiers and DNRA bacteria; (B) relative abundance of DNRA bacteria (to the total  
673 of denitrifiers and DNRA bacteria) and contribution of DNRA in nitrate partitioning at different  
674 influent COD/N ratios (at influent nitrate concentration of 1000  $\mu\text{M}$ ). The black triangles represent the  
675 measured DNRA biomass fraction (at influent nitrate concentration of 11790  $\mu\text{M}$  [13])

676

677

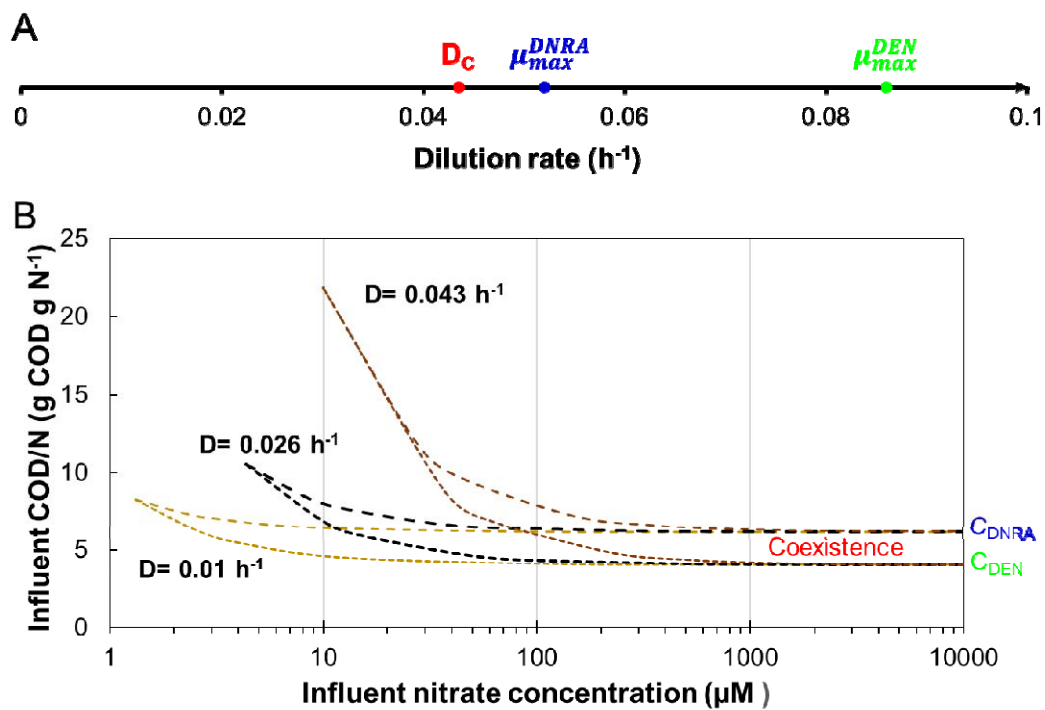


678

679 **Figure 4.** The boundary influent COD/N ratios at different influent nitrate concentrations. The regions  
680 correspond to the regions with the same numbers in Fig. 2. Points a, b, c, and d are supply points with  
681 the same COD/N ratio but different nitrate concentrations (detailed in Fig. S5).

682

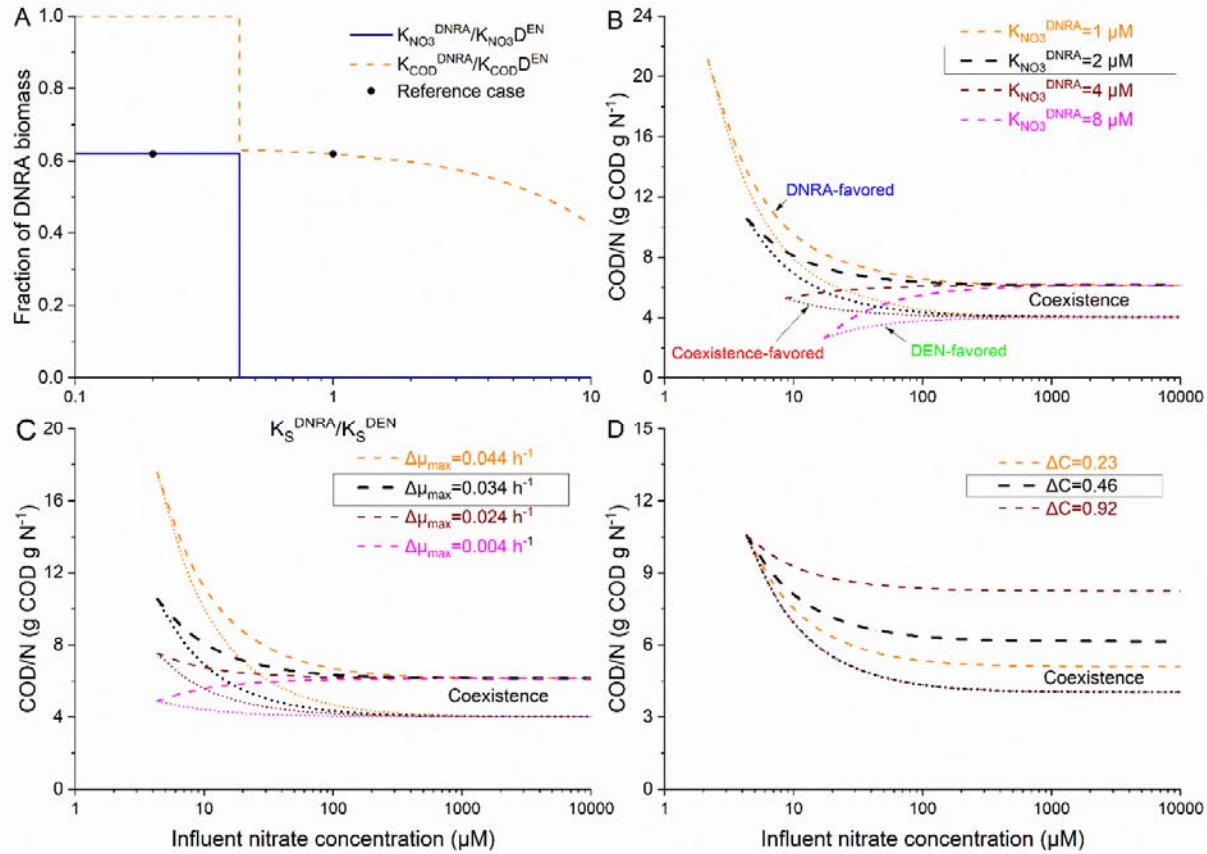
683



684

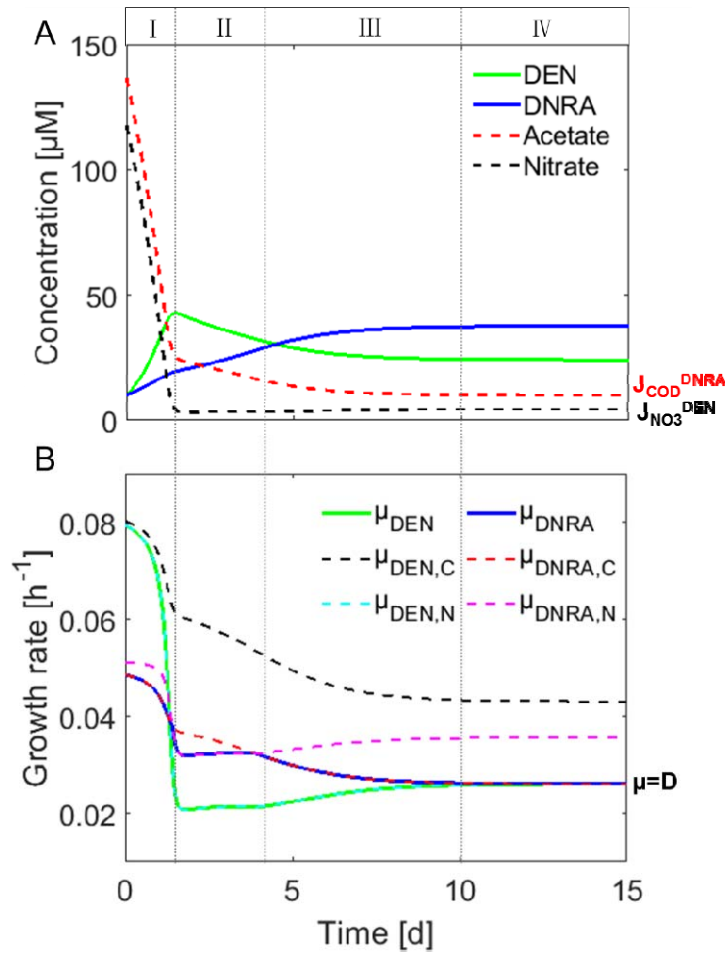
685 **Figure 5.** Impact of dilution rate on (A) possible competition outcomes; (B) the boundaries of  
686 coexistence.





687

688 **Figure 6.** Impact of kinetic and stoichiometric parameters on the boundaries for coexistence: (A) the ratio of the affinity constants of the two species for the  
 689 same resource (conditions: influent COD/N=5.3 with 1000 μM nitrate and fixed affinity constants for denitrifiers); (B) affinity for nitrate, expressed as  
 690  $K_{NO_3}^{DNRA}$ , with fixed  $K_{NO_3}^{DNRA}/K_{NO_3}^{DEN}$ ; (C) maximum growth rate, expressed as  $\Delta\mu$  (i.e.,  $\mu_{max}^{DEN} - \mu_{max}^{DNRA}$ ) and (D) yield coefficient, expressed as  $\Delta C$  (i.e.,  
 691  $C_{DNRA} - C_{DEN}$ ). The values in the box were default values at the reference case.



692

693 **Figure 7.** Trajectories of: (A) resources and species concentrations; (B) calculated growth rate in a  
694 chemostat fed with acetate and nitrate at a COD/N ratio of 5.3, under which stable coexistence of DEN  
695 and DNRA was observed [13] and predicted (this study). The DEN and DNRA species were initially  
696 equally presented in a chemostat.

697

698

699 **Table 1.** Typical nitrate concentrations in several ecosystems

<b>Ecosystems</b>	<b>NO<sub>3</sub><sup>-</sup> (μM)</b>	<b>Source</b>
Seawater	< 30	[29]
Groundwater	< 806	[30]
Surface water	< 161	[31]
Marine sediments	3.7-17.8	[32]
Terrestrial ecosystems <sup>a</sup>	0.01-4.96 <sup>b</sup>	[4]
WWTPs	< 4200 <sup>c</sup>	[33]

a: Forest, grassland, riparian;

b: in μM /g soil

c: assuming all the influent ammonium is converted to nitrate for a medium strength municipal wastewater

700